

Aerothermodynamic Modeling of Hydrogen-Fuelled Dual Bypass Turbofan Engine

¹Alex. A. Avwunuketa²Oyinkansola O. Alade

^{1,2}Aeronautical and Astronautical Engineering Department,
College of Engineering,
Afe Babalola University
Ado-Ekiti, Ekiti State, Nigeria.
Alex. A. Avwunuketa

Date of Submission: 01-04-2026

Date of Acceptance: 11-04-2026

ABSTRACT: Aircraft fuel price has increased therefore aircraft economy has become more significant. In addition, recent years have seen many aircraft ideas on account of the high cost of fuel and the necessity to deal with the environmental issues. The literature on the issue seems to reveal that hydrogen is the most noticeable alternative fuel. However, this study puts forward the use of hydrogen powered aircraft as a possible solution to the environmental anomalies induced by conventional aircraft fuelled with fossil fuels. Analysis was conducted to determine how flight altitude, flight-Mach number, intake air, and hydrogen fuel affect thrust specific fuel consumption and specific thrust of a turbofan engine with dual bypass ratio. Fuel consumption and pollutant generation rates from aero engines are the two extreme problems. The results obtained from this work, shows that there is an 8.5 % decrease in TSFC with the increase of 36.8 % for the first bypass ratio and 100% for the second bypass ratio, TFSC decreases of 4.7 %. The results and suggested methodology presented in this research could be used as a base for overall consideration of the dual bypass engine relying on hydrogen fuel. The aircraft engine suggested design is the required decision for the aviation industry future in terms to increase energy efficiency and to have less harmful environmental impact.

KEYWORDS: Aircraft, Bypass, Hydrogen, Thrust, Turbofan.

I. INTRODUCTION

Environmental limitations on fossil fuels have resulted in extensive study on efficiency and optimization of gas turbine engines. Current works by [1] are based on the application of artificial intelligence (AI). Gas turbine (GT) is one of the most useful aircraft engine types. The simplicity and as well as the adaptability of gas turbine models make them widely used in research to estimate

performance over a variety of operating conditions. These frameworks rely on the use of a physical model that is accurate and predictable because it helps in fault identification, running schedules optimization, and thermal efficiency analysis. In many subsystems where sensor manipulation is difficult, such as high-pressure turbines (HPT), it is very helpful to have an accurate model. The model can be reliably used to estimate the same state variables as transducers. Combination of data fusion methods and latest development of neural networks have been shown to effectively improve the entire system mathematical model [2].

Brayton cycle gas turbines are both extensively used in aerospace propulsion systems and electric power plants. Their advantages include quicker startup times, improved thermal efficiency, robustness and reliable systems [3]. Gas turbines are widely used in aircraft engines due to their adjustable power and range of thrust forces. Although the turbojet is the most basic form of jet engine. The turbofan, turboprop, and turboshaft are the most widely utilized gas turbine systems [4]. Turbofan engine is the most used gas turbine engine for aircrafts designed to be used for commercial purpose because it has higher propulsive efficiency and low fuel consumption compared to turbo jet engine [5]. Turbofan engines are classified based on the bypass ratio, number of turbines, number of flow channels, and flow mixing system. Energy, economic, and environmental (3E) analysis is crucial for turbofan engine design and modification. The JT15D turbofan engine performance was evaluated in terms of principles of energy, sustainability and exergy by [6]. They discovered that in order to generate 315.9 N s/kg of specific thrust, the engine needs 15.8 g/kN/s of thrust-specific fuel consumption (TSFC). [7] assessed ammonia performance in civil aircraft as a carbon-free fuel. They researched the propulsion of the Airbus A350-1000. The use of ammonia as fuel necessitates the modification or

redesign of the engine. Ammonia-powered aircraft have the potential to reduce global warming by up to 75%, which makes them a promising way to improve the environmental aspects of turbofan engines. In addition, ammonia powered systems can have smaller, more compact cores as well as higher thermal efficiency according to the technology. Although ammonia is not yet being fairly adopted due to its hazardous nature. Jet-A1 fuel was used by [8] in investigating a CFM56-3 turbofan engine model. The energy efficiency, exergy efficiency and the waste energy ratio were calculated under different operating condition by the authors. Furthermore, the engine environmental impact and the economic factor were also calculated. The work calculates the fuel specific energy cost, the engine specific energy cost and the product specific energy cost.

Therefore, the optimal point should be determined considering all these parameters Energy, exergy, environment as well as the economy. Recent study has considered optimization of these analyses for turbofans and other gas turbine engines. In order to improve the performance of various systems, this work uses multi-objective functions, sophisticated algorithms, sensitivity analysis, uncertainty quantification and experimental design. The TF30-P414 turbofan engine performance was examined by [9], it worked on the effects of flight altitude and flying Mach number on thermal efficiency, thrust, and fuel mass flow rate. At altitude of 11.24km and a Mach number of 1.944, thermal efficiency was maximized at 32.64%.

A GE90 turbofan engine powered with hydrogen and hydrocarbon fuel, as published by [10]. An evolutionary algorithm was applied to determine the optimal bypass and fan pressure ratios with regard to performance, cost and environmental considerations. The improved hydrogen turbofan engine, generated higher net thrust force, higher thermal efficiency, lower nitrogen oxide (NOx) emissions, and lower thrust specific fuel consumption. In terms of specific mass flow rate of fuel consumed and thrust produced, by the cruising phase, the overall nitrogen oxide emissions were reduced by 68.25%. In addition to optimization, ML techniques are useful for enhancing operational performance of aero derivative engines [11-16]

The Mixed-Flow Turbofan (MFT) engine model was used to make aircraft emission predictions was emphasized by [1]. Initially, convolutional long-short term memory (LSTM) is applied for estimating the fuel flow rate, NOx and CO emission indices. A hybrid Convolutional Neural Network (CNN-LSTM) model is used to improve the estimates. The hybrid model outperforms the LSTM model in fuel

flow estimates, with a higher R2 for both phases. The proposed CNN-LSTM model can better estimate key characteristics of gas turbine engines.

During the takeoff phase [14] employed support vector regression (SVR) and LSTM approaches to predict emissions indexes (EIs) and the fuel flow of aircraft engines. The laws of thermodynamics are used to calculate exergy-environmental indicators such as the environment effect factor, the wasted exergy ratio and the energy efficiency. When SVR is used, the coefficient of determination (R2) of the emission index of carbon monoxide (EI-CO) and the emission index of nitrogen oxides (EI-NOx) is higher than the coefficient of determination of the emission index of hydrocarbons (EI-HC) [15]. Precise models of environmental and emission characteristics help forecast these aspects for upcoming engine designs [16].

Variable cycle engines (VCEs) have huge promise to create future aircraft models. They fix the problems that come with standard low-bypass mixed turbofan engines [17]. To get better performance in various flight situations, you need the variable cycle engine to be able to adjust those bypass ratios on the fly. That's where the cycle analysis of a dual-bypass turbofan engine comes in useful for planning a variable cycle engine. Research by [18] looked at an adaptive cycle engine (ACE) candidate for a flight engine. They analyzed both single bypass mode (SBM) and dual bypass mode (DBM). The study found that the SFC value for the ACE model is 17.41 g/kN. s in DBM and 40.45 g/kN. s in SBM. That revealed that the engine would have better performance in different flight conditions.

[19] Research on mixed-flow turbofans has shown that the VCE model can be used to assess the performance of these engines. In one study, the cycle equations of a mixed-flow turbofan with an afterburner were used to create the VCE model. That investigation found that the energetic stability index, measure of how stable an engine is in terms of its energy use varies between 0.14 and 0.51 for DBM and 0.26 and 0.38 for SBM. One of the benefits of the VCE model is that it allows you to adjust the by-pass ratio by combining different thermodynamic cycles like turbojet and turbofan into one system.

That study compared the F100 engine performance to the VCE in off-design situations. It looked at how the working cycle affects engine performance and sustainability measures. Most research into mixed-flow turbofans does focus on how different factors

affect them. But there is still a real need for research on energy, environmental and economic assessments and on using AI techniques and multi-objective function optimization to introduce new dual-bypass turbofans [1]. According to recent studies, the main fuels for aero-derivative gas turbines are hydrogen [21-23], biodiesel [24-25], and kerosene [26-28]. Recent studies have shown that these are the most promising options. There is a lot of research on the economic, environmental and energy-related impacts of different factors on mixed-flow turbofans. That's where the VCE model comes in. By assessing the performance of these engines, we can better understand how to make them more sustainable and efficient [29]

Recent years have seen a huge increase in interest in emissions reduction and combustion efficiency, similar to dual-fuel engine concepts. Research on hydrogen-diesel dual-fuel engines by [30] and [31] revealed that injecting hydrogen into diesel fuels might significantly lower emissions of hydrocarbons and carbon monoxide, improving combustion efficiency. The best way to achieve net-zero emissions is through hydrogen propulsion; the most practical option for airplanes with weight and volume constraints is liquid hydrogen storage. However, the energy needed to liquefy hydrogen would raise the price of hydrogen fuel for aircraft. NO_x emissions also grow with an increase in combustion temperature, which is always a problem for dual-fuel engines. These factors are solely due to dual-fuel engines impracticability in aircraft systems. hydrogen was used as the main fuel in a study because it was less expensive [32]. Pure hydrogen also serves as an economically and ecologically viable substitute for the widely utilized liquid petroleum-based fuels in aircraft. The economic benefits include a higher energy density per unit volume to lower fuel and storage costs, as well as generally lower expenses compared to other fuel. Additionally, hydrogen burns cleaner, which may result in lower engine maintenance expenses for aircraft.

This research uses a machine learning-based algorithm to forecast and optimize additional parameters (thrust-specific nitrogen oxide production rate, thrust-specific fuel consumption cost), which sets it apart from earlier work, whereas the F135 research by [33], focused only on predicting several functional parameters. The effects of turbine inlet temperature, high-pressure compressor compression ratio, fan pressure ratio, low-pressure compressor compression ratio, and first and second bypass ratios on conceptual parameters like thrust-specific carbon monoxide production rate (TSCO), TSF, TSFCC, and TSNOX are investigated in this study. The novelties and innovation of this study focus on the energy, environment and economy analysis and optimization of low-emission hydrogen fuel dual-bypass turbofan engine.

II. METHODOLOGY

This study examines such an engine arrangement to include: A part of the fan flow enters the mixer via the first bypass channel, a part of the flow from the low-pressure compressor enters the mixer via the second bypass channel. The low-pressure turbine outlet flow is mixed with the first and second bypass flows in the mixer before it is discharged into environment through the nozzle.[34]. At the same time, the high-pressure compressor dense stream of air will pass through combustion chamber wherein fuel is burnt. Combustion products entering them cause both of them to rotate as a high pressure and low-pressure turbines respectively. The high-pressure turbine drives the high-pressure compressor and the low-pressure turbine drives the low-pressure compressor and fan. The configuration of the turbofan engine is shown in Figure 1.

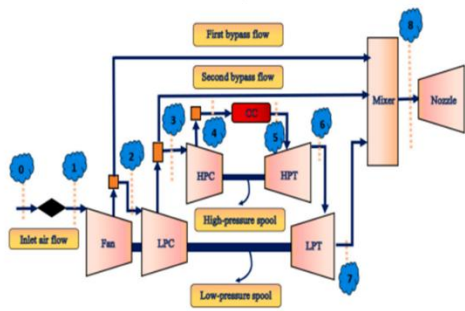


Figure 1: Dual-bypass turbofan configuration [35]

$$\text{bypass ratio} = \frac{\text{mass flow through the bypass section}}{\text{mass flow through the core section}} \quad 1$$

At the low-pressure compressor inlet is:

$$\dot{m}_0 = \dot{m}_2 + \dot{m}_{b1} \quad 2$$

$$\dot{m}_2 = \frac{\dot{m}_0}{(1 + \alpha_1)} \quad 3$$

Where \dot{m}_0 is the freestream engine intake air mass and \dot{m}_2 is the hot air passing through the hot section of the low-pressure section and α_1 bypass ratio of the first bypass section.

At the high-pressure section

$$\dot{m}_0 = \dot{m}_2 + \dot{m}_3 + \dot{m}_{b2} \quad 4$$

$$\dot{m}_{b2} = \alpha_2 \dot{m}_3 \quad 5$$

$$\dot{m}_3 = \frac{\dot{m}_0}{\alpha_2} \left[\frac{2 + \alpha_1}{1 + \alpha_1} \right] \quad 6$$

\dot{m}_3 is the hot air passing through the hot section of the high-pressure section and α_2 bypass ratio of the second bypass section. The mass flow rates of air through the first bypass channel (\dot{m}_{b1}) and the second or dual bypass channel (\dot{m}_{b2}) respectively.

The total inlet output temperature (T_{t1}) and pressure (P_{t1}) are computed as follows.

$$T_{t1} = T_0 \left[1 + \frac{\gamma_d - 1}{2} M_0^2 \right] \quad 7$$

$$P_{t1} = P_0 \left[\frac{T_{t1}}{T_0} \right]^{\frac{\gamma_d}{\gamma_d - 1}} \quad 8$$

$$P_{t1} = P_0 \left[1 + \frac{\gamma_d - 1}{2} M_0^2 \right]^{\frac{\gamma_d}{\gamma_d - 1}} \quad 9$$

M_0 and γ_d are for the flight Mach number and specific heat capacity ratio of incoming air respectively. The static air temperature and pressure of incoming air are T_0 and P_0 respectively.

The fan air pressure ratio is (π_F).

Fan output flow total pressure is:

$$P_{t2} = \pi_{Fan} \times P_{t1} \quad 10$$

The fan output flow total temperature (T_{t2}) is determined.

$$T_{t2} = \frac{T_{t1}}{\eta_{Fan}} \left[(\pi_{Fan})^{\frac{\gamma_{Fan} - 1}{\gamma_{Fan}}} - 1 \right] + T_{t1} \quad 11$$

where (η_{Fan}) the fan isentropic efficiency and (γ_{Fan}) the specific heat capacity ratio of air on the fan.

The low-pressure compressor output flow total pressure (P_{t3}) and temperature (T_{t3}) are:

$$(\pi_{LPC}) = \frac{P_{t3}}{P_{t2}} \quad 12$$

$$T_{t3} = \frac{T_{t2}}{\eta_{LPC}} \left[(\pi_{LPC})^{\frac{\gamma_{LPC} - 1}{\gamma_{LPC}}} - 1 \right] + T_{t2} \quad 13$$

Where (π_{LPC}) is the low-pressure compressor ratio, (η_{LPC}) low-pressure compressor isentropic efficiency and (γ_{LPC}) specific heat capacity ratio of air on low pressure compressor.

The power input from the low-pressure compressor is calculated as;

$$W_{LPC} = \dot{m}_2 C_{pLPC} \frac{T_{t2}}{\eta_{LPC}} \left[(\pi_F)^{\frac{\gamma_{LPC} - 1}{\gamma_{LPC}}} - 1 \right] \quad 14$$

The production power of a low-pressure turbine (W_{LPT}) is obtained:

$$W_{LPT} = \dot{m}_6 C_{pLPT} (T_{t6} - T_{t7}) \quad 15$$

$$\dot{m}_6 = \dot{m}_5 \quad 16$$

Where C_{pLPT} is the specific heat of the flow through the low-pressure turbine and \dot{m}_6 is the mass flow rate through the turbine. W_{LPT} is the power extracted from the low-pressure turbine.

$$\pi_{LPT} = \left[1 - \frac{1}{\eta_{LPT}} (1 - \tau_{LPT}) \right]^{\frac{\gamma_{LPT}}{\gamma_{LPT} - 1}} \quad 17$$

$$\pi_{LPT} = \frac{P_{t7}}{P_{t6}} \quad 18$$

$$\tau_{HPT} = \frac{T_{t7}}{T_{t6}} \quad 19$$

Where (π_{LPT}) is the low-pressure turbine pressure ratio, (η_{LPT}) low-pressure turbine isentropic efficiency and (γ_{LPT}) specific heat capacity ratio of air on low pressure turbine.

The low-pressure turbine drives the low-pressure compressor and the fan.

$$\dot{W}_{LPT} = \dot{W}_{LPC} + \dot{W}_F \quad 20$$

$$\dot{W}_F = \dot{m}_0 C_{pFan} \frac{T_{t1}}{\eta_{Fan}} \quad 21$$

$$\pi_F = \frac{P_{t2}}{P_{t1}} \quad 22$$

Where (π_{Fan}) is the fan pressure ratio, (η_{HPT}) fan isentropic efficiency and (C_{pFan}) specific heat capacity ratio of air on the fan.

The high-pressure compressor output flow total pressure (P_{t4}) and total temperature (T_{t4}) are:

$$(\pi_{HPC}) = \frac{P_{t4}}{P_{t3}} \quad 23$$

$$T_{t4} = \frac{T_{t3}}{\eta_{HPC}} \left[(\pi_{HPC})^{\frac{\gamma_{HPC}-1}{\gamma_{HPC}}} - 1 \right] + T_{t3} \quad 24$$

The power consumption of a high-pressure compressor is calculated as;

$$\dot{W}_{HPC} = \dot{m}_3 C_{HLPC} \frac{T_{t3}}{\eta_{HPC}} \left[(\pi_F)^{\frac{\gamma_{HPC}-1}{\gamma_{HPC}}} - 1 \right] \quad 25$$

Where (π_{HPC}) is the high-pressure compressor ratio, (η_{HPC}) high-pressure compressor isentropic efficiency and (γ_{HPC}) specific heat capacity ratio of air on high-pressure compressor.

The combustion chamber exhaust total pressure (P_{t5}) computed as follows:

$$P_{t5} = P_{t4} - \Delta P_{cc} \quad 26$$

Where (ΔP_{cc}) is change in pressure as result of combustion

The turbine inlet temperature (TIT) and the combustion chamber exhaust flow temperature (T_{t5}) are equal, and the high-pressure turbine production (\dot{W}_{HPT}) is ascertained as follows:

$$T_{t5} = TIT \quad 27$$

$$\dot{W}_{HPT} = \dot{m}_5 C_{PHPT} (T_{t5} - T_{t6}) \quad 28$$

$$\dot{m}_5 = \dot{m}_4 + \dot{m}_f \quad 29$$

Where C_{PHPT} is the specific heat of the flow through the high-pressure turbine and \dot{m}_3 is the mass flow rate through the turbine. \dot{W}_{HPT} is the power extracted from the high-pressure turbine.

The total exit pressure from the high-pressure turbine (P_{t6}) is determined by total inlet temperature of the high-pressure turbine (T_{t5}) .

$$\pi_{HPT} = \left[1 + \frac{1}{\eta_{HPT}} (1 - \tau_{HPT}) \right]^{\frac{\gamma_{HPT}}{\gamma_{HPT}-1}} \quad 30$$

$$\pi_{HPT} = \frac{P_{t6}}{P_{t5}} \quad 31$$

$$\tau_{HPT} = \frac{T_{t6}}{T_{t5}} \quad 32$$

Where (π_{HPT}) is the high-pressure turbine pressure ratio, (η_{HPT}) high-pressure turbine isentropic efficiency and (γ_{HPT}) specific heat capacity ratio of air on high-pressure turbine.

Fuel consumption mass flow rate (\dot{m}_f) is calculated as:

$$\dot{m}_f = \frac{\dot{m}_3 C_{pcc} (T_{t5} - T_{t4})}{LHV_f \eta_{cc}} \quad 33$$

The specific heat capacity at constant pressure of the incoming air in the combustion chamber, the low heat value of the unit of fuel mass, and the combustion efficiency are denoted by C_{pcc} , LHV_f and η_{cc} respectively.

Applying mass flow conservation:

$$\begin{aligned} \text{Mass flow into the mixer} \\ &= \text{mass flow out of mix} \quad 34 \\ \dot{m}_8 &= \dot{m}_{b1} + \dot{m}_{b2} + \dot{m}_7 \quad 35 \end{aligned}$$

The energy conservation principle is used to compute the temperature of the mixer's output flow (T_{t8}) ;

$$T_{t8} = \frac{\dot{m}_{b1} C_{pb1} T_{t2} + \dot{m}_{b2} C_{pb2} T_{t3} + \dot{m}_7 C_{p7} T_{t7}}{C_{p8} (\dot{m}_{b1} + \dot{m}_{b2} + \dot{m}_7)} \quad 36$$

where T_{t7} , T_{t2} , T_{t3} is total temperature from low-pressure turbine, first bypass air and second bypass air respectively. C_{p7} , C_{pb1} and C_{pb2} are specific heat capacity of air from low-pressure turbine, air from first bypass and air from second bypass respectively.

The output velocity of the nozzle (V_9) is calculated as;

$$V_9 = \left(2 \eta_n C_{p8} T_{t8} \left[1 - (\pi_n)^{\frac{\gamma_n-1}{\gamma_n}} \right] \right)^{0.5} \quad 37$$

where η_n , C_{p8} , T_{t8} , π_n and γ_n are nozzle isentropic efficiency, specific heat capacity of output air, total output temperature, nozzle pressure ratio and specific heat ratio of air at nozzle respectively.

The engine thrust is the primary power source that propels aircraft to satisfy force requirements during flight, particularly during takeoff. It helps the aero vehicle overcome the drag force caused by the air acting on its surface. For mixed flow turbofan engine with dual bypass, the thrust is calculated as:

$$\begin{aligned} T &= \dot{m}_0 \left[(1 + f + (\alpha_1 + \alpha_2)) V_9 - (1 + (\alpha_1 + \alpha_2)) V_0 \right] \\ &\quad + A_9 (P_9 - P_0) \quad 38 \end{aligned}$$

Where f is the fuel ratio.

Table 1 shows the dual bypass turbofan engine cycle design cycle parameters that were investigated in this study.

Table 1: Design cycle parameters of dual-bypass turbofan engine [36]

Parameters	Symbol	Values	Units
Inlet air mass flow rate at Take-off	\dot{m}_0	152	kg/s
Fan pressure ratio	π_F	5.3	-
Low-pressure compressor pressure ratio	π_{LPC}	4.5	-
High-pressure compressor pressure ratio	π_{HPC}	8.0	-
Turbine inlet temperature	T_{t5}	2130	K
First bypass ratio	α_1	0.6	-
Second bypass ratio	α_2	1.3	-
Isentropic efficiency of the fan	η_{Fan}	0.81	-
Isentropic efficiency of Low-pressure compressor	η_{LPC}	0.82	-
Isentropic efficiency of High-pressure compressor	η_{HPC}	0.85	-
Isentropic efficiency of Low-pressure turbine	η_{LPT}	0.89	-
Isentropic efficiency of High-pressure turbine	η_{HPT}	0.90	-
Combustion chamber efficiency	η_{CC}	0.96	-
Hydrogen fuel	H_2	129	MJ/kg

Table 2: bypass ratio with TSF and TSFC

α_1	α_2	TSF (N.s/kg)	TSFC (kg/kN.s)
0	0	300	26
0.1	0.1	400	27
0.2	0.2	600	28
0.3	0.3	700	29
0.4	0.4	800	30
0.5	0.5	900	31
0.6	0.6	1000	33

III. RESULT AND DISCUSSIONS

When embarking on the conceptual design of a turbofan engine and its efficient operation, it is necessary to define the right parameters for determining the flight conditions. To meet as much

power as possible for a commercial supersonic aircraft, the supersonic cruise concept was used as a design basis for development of the dual bypass turbofan engine cycle. This work has modeled and examined a turbofan engine without an afterburner. Actually, creating a dual-bypass turbofan engine with hydrogen fuel and with supersonic cruise capabilities for use in commercial flights was one of the objectives of this study. Supersonic cruise capability literally means that the engine can reach supersonic speed without the need for an afterburner. According to [37], this condition suggested a Mach number of 1.8 and an altitude of 17,000 meters with respect to sea level. These factors are specific to this aircraft and form the foundation for further research that may examine the design costs, efficiency, and environmental friendliness. Furthermore, to arrive at the engine performance under such situation, the engine specific thrust, the specific emissions of carbon monoxide and nitrogen oxides as a function of thrust, and the specific fuel consumption per unit of thrust at this supersonic condition are to be determined. When it comes to specific fuel consumption, dual bypass engines using hydrogen fuel, perform better than conventional turbofan engines. This results in lower fuel costs and lower specific production rates of pollutants like NOx and CO. This study analyzes and maximizes a dual-bypass turbofan engine utilizing hydrogen as fuel with regard to energy-exergy and environmental performance.

Specific thrust may be defined as important parameter in assessing the performance of propulsion systems. It will analyze how specific thrust changes with changes in design, operating parameters, or types of fuel used. It will examine the effects of modifications to the design, operational settings, or fuel types on a given thrust. This parameter may require formulas or other computations, simulations or experiments giving performance data to establish standards to which this parameter relates, and with sufficient understanding of the absolute thrust force, it is possible to develop further environmentally friendly and energy efficient propulsion systems. The impact of the first and second bypass ratio parameters on two functional parameters of the specific thrust force (TSF) and the specific thrust fuel consumption

(TSFC) were investigated under the presumption of using hydrogen fuel, at an altitude of 17,000 meters above sea level, and with a Mach number of 1.8.

Figures 5 and 6, shows how a dual-bypass turbofan engine specific thrust force (TSF) varies with the first and second bypass ratios.

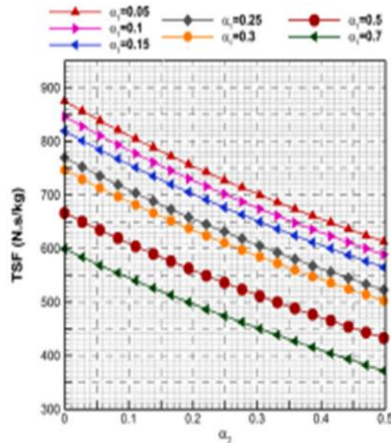


Figure 5: TSF with bypass ratio (α)

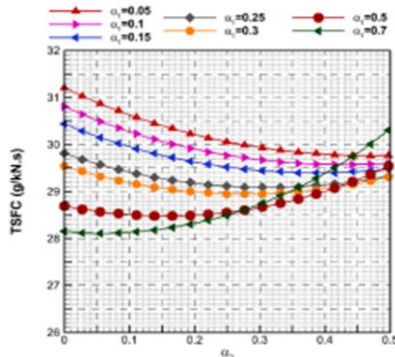


Figure 5: TSFC with second bypass ratio (α)

A 40 percent rise in the first bypass ratio was also observed in the results when the second bypass ratio was zero and TSF 10.05% decreased. When the second bypass ratio is 0.5 and the first bypass ratio is increased by 40%, TSF drops to roughly 14%. Also, when the first bypass ratio is 0.25 and the second bypass ratio increases by 37.5%, the TSF decreases by 0.62%.

However, TSFC increased by 0.9% when the first bypass ratio was increased by 20% within the range of 0.25 to 0.35, provided that the second bypass ratio is equal to 0. The results also showed that, if the first bypass ratio is 0.1 and the second bypass ratio is increased by 100% within the range

of 0–0.3, the TSFC decreases by 4.73%. The result shows that TSFC would rise by about 2% in the event that the first bypass ratio value was 0.5 and the second bypass ratio increased by 100% in the range of 0 to 0.4. According to the findings, the TSFC trend will shift from declining to rising at a point that corresponds to the first bypass of about 0.5.

IV. CONCLUSION

The study investigated how design characteristics affected a dual-bypass turbofan engine that utilize hydrogen fuel with regard to performance in a supersonic commercial aircraft under nominal flight conditions. Thrust-specific fuel consumption (TSFC), and specific thrust force (TSF) were the main subjects of the analysis. The key findings shows that a 38.6 % increase in the first bypass ratio (α_1), there is 10% reduction in TSFC, when the second bypass ratio (α_2) is set to zero. Under the same conditions, TSF decreases by 10.2 %. Also, a 100% increase in the second bypass ratio (α_2) from 0 to 0.4 reduces TSFC by 4.65 % when α_1 is 0.1. For α_1 values above 0.3, increasing α_2 leads to a sharp increase in TSFC.

References

- [1] J. Zhang, H. Tang and M. Chen, "Robust design methodologies to the adaptive cycle engine system performance: preliminary analysis," *Energy Procedia*, vol. 158, pp. 1521-1529, 2019.
- [2] D. Tan, Y. Wu, J. Lv, J. Li, X. Ou, Y. Meng, G. Lan, Y. Chen and Z. Zhang, "Performance optimization of a diesel engine fueled with hydrogen/biodiesel with water addition based on the response surface methodology," *Energy*, vol. 263, no. 125869, 2023.
- [3] Z. Zhang, S. Wang, M. Pan, J. Lv, K. Lu, Y. Ye and D. Tan, "Utilization of hydrogen-diesel blends for the improvements of a dual-fuel engine based on the improved Taguchi methodology," *Energy*, vol. 292, no. 130474, 2024.
- [4] P. Liu, T. Yang, H. Zheng, X. Huang, X. Wang, T. Qiu and S. Ding, "Thermodynamic analysis of power generation thermal management system for heat and cold exergy utilization from liquid

- hydrogen-fueled turbojet engine," *Applied Energy*, Vols. 365, no. 123290, 2024.
- [5] M. Sabzehali, A. Rabiee, M. Alibeigi and A. Mosavi, "Predicting the energy and exergy performance of F135 PW100 turbofan engine via deep learning approach," *Energy Conversion and Management*, vol. 265, no. 115775, 2022.
- [6] E. Baharozu, G. Soykan and M. Ozerdem, "Future aircraft concept in terms of energy efficiency and environmental factors," *Energy*, vol. 140, pp. 1368-1377, 2017.
- [7] H. Chen, C. Cai, J. Luo and H. Zhang, "Flow control of double bypass variable cycle engine in modal transition," *Chinese Journal of Aeronautics*, vol. 35, no. 10, pp. 134-147, 2022.
- [8] D. Verstraete, "Long range transport aircraft using hydrogen fuel," *International Journal of Hydrogen Energy*, vol. 38, no. 34, pp. 14824-14831, 2013.
- [9] H. Aygun, O. Dursun and S. Toraman, "Machine learning based approach for forecasting emission parameters of mixed flow turbofan engine at high power modes," *Energy*, no. 271, pp. 23-47, 2023.
- [10] S. Kim, K. Kim and C. Son, "A new transient performance adaptation method for an aero gas turbine engine," *Energy*, vol. 193, no. 116752, 2020.
- [11] D. Mohaddes, C. Chang and M. Ihme, "Thermodynamic cycle analysis of superadiabatic matrix-stabilized combustion for gas turbine engines," *Energy*, vol. 207, no. 118171, 2020.
- [12] E. Ogur, A. Koç, H. Yağlı, Y. Koç and O. Kose, "Thermodynamic, economic, and environmental analysis of a hydrogen-powered turbofan engine at varying altitudes," *Int. J. Hydrogen Energy*, vol. 55, p. 1203-1216, 2024.
- [13] A. Avwunuketa, M. Bonet, M. Adamu, U. Haruna and O. Fadenipo, "Performance, Characterization and Evaluation of Axial Flow Turbine Engine," *International Journal of Advances in Scientific Research and Engineering (IJASRE)*, vol. 5, no. 10, pp. 124 - 131, 2019.
- [14] O. Balli, N. Caliskan and H. Caliskan, "Aviation, energy, exergy, sustainability, exergoenvironmental and thermoeconomic analyses of a turbojet engine fueled with jet fuel and biofuel used on a pilot trainer aircraft," *Energy*, vol. 263, no. 126022, 2023.
- [15] S. Sasi, C. Mourouzidis, D. Rajendran, I. Roumeliotis, V. Pachidis and J. Norman, "Ammonia for civil aviation: a design and performance study for aircraft and turbofan engine," *Energy Conversion. Management.*, vol. 307, no. 118294, 2024.
- [16] P. Korba, O. Balli, H. Caliskan, S. Al-Rabeei and U. Kale, "Energy, exergy, economic, environmental, and sustainability assessments of the CFM56-3 series turbofan engine used in the aviation sector," *Energy*, vol. 269, no. 126765, 2023.
- [17] S. Farahani, M. Alibeigi and M. Sabzehali, "2021. Energy and exergy analysis and optimization of turbofan engine-TF30-P414.," *Iranical Journal of Energy and Environment.*, vol. 12, pp. 307-317, 2021.
- [18] P. Derakhshandeh, A. Ahmadi and R. Dashti, *International Journal of Hydrogen and Energy*, vol. 46, p. 3303-3318, 2021.
- [19] C. Fujio and H. Ogawa, "Deep-learning prediction and uncertainty quantification for scramjet intake flowfields," *Aerospace Science & Technology*, vol. 130, no. 107931, 2022.
- [20] Z. Wei, Y. Ma, N. ang, S. Ruan and C. Xiang, "Reinforcement learning based power management integrating economic rotational speed of turboshaft engine and safety constraints of battery for hybrid electric power system," *Energy*, vol. 263, no. 263, 2023.
- [21] B. An, M. Sun, Q. Zhao, L. Yang, D. Yang, Y. Huang, P. Li, J. Wang and Y. Yang, "Analysis of the combustion modes in a rocket-based combined cycle combustor using unsupervised machine learning methodology," *Physics of Fluids*, vol. 36, 2024.
- [22] O. Dursun, S. Toraman and H. Aygun, "Deep learning approach for prediction of exergy and emission parameters of commercial high by-pass turbofan engines," *Environmental Science & Pollution Control Services*, vol. 30, p. 27539-27559, 2023.
- [23] M. Castro-Cros, M. Velasco and C. Angulo, "Machine-Learning-Based Condition Assessment of Gas Turbines," *A Review. Energies*, vol. 14, 2021.
- [24] M. Sabzehali, A. Hossein Rabiee, M. Alibeigi and A. Mosavi, "Predicting the energy and exergy

- performance of F135 PW100 turbofan engine via deep learning approach.," *Energy Conversion & Management*, vol. 265, 2022.
- [25] A. Avwunuketa, H. O. Musa-Basheer and O. Erhinyodavwe, "Characteristics Investigation of Combustion Properties of Electrofuels For Aerospace Application," in *2024 International Conference on Science, Engineering and Business for Driving Sustainable Development Goals (SEB4SDG)*, Ado-Ekiti, 2024.
- [26] J. Junchao, C. Min and C. Hailong, "Matching mechanism analysis on an adaptive cycle engine," *Chinese Journal of Aeronautics*, vol. 30, no. 2, pp. 706-718, 2017.
- [27] M. Chen, J. Zhang and H. Tang, "Interval analysis of the standard of adaptive cycle engine component performance deviation," *Aerospace Science and Technology*, vol. 81, pp. 179-191, 2018.
- [28] A. Dinc and I. Elbadawy, "Global warming potential optimization of a turbofan powered unmanned aerial vehicle during surveillance mission," *Transportation Research Part D: Transport and Environment*, vol. 85, no. 102472, 2020.
- [29] A. Patrao, I. Jonsson, C. Xisto, A. Lundbladh, M. Lejon and T. Grönstedt, "The heat transfer potential of compressor vanes on a hydrogen fueled turbofan engine," *Applied Thermal Engineering*, vol. 236, no. C, pp. Volume 236., 2024.
- [30] P. Boomadevi, V. Paulson, S. Samlal, M. Varatharajan, M. Sekar, M. Alsehli, A. Elfasakhany and S. Tola, "Impact of microalgae biofuel on microgas turbine aviation engine: A combustion and emission study," *Fuel*, vol. 302, no. 121155, 2021.
- [31] O. Balli, E. Ozbek, S. Ekici, A. Midilli and T. H. Karakoc, "Thermodynamic comparison of TF33 turbofan engine fueled by hydrogen in benchmark with kerosene," *Fuel*, vol. 306, no. 121686, 2021.
- [32] E. Ozbek, G. Yalin, M. Karaoglan, S. Ekici, C. Colpan and T. Karakoc, "Architecture design and performance analysis of a hybrid hydrogen fuel cell system for unmanned aerial vehicle," *International Journal of Hydrogen Energy*, vol. 46, no. 30, pp. 16453-16464, 2021.
- [33] A. Avwunuketa, F. Chieze and J. Obodo, "A Review of Vehicles using Hydrogen Internal Combustion Engines," in *International Conference on Science, Engineering and Business for Driving Sustainable Development Goals (SEB4SDG)*, Nigeria, 2024.
- [34] B. Doğan, M. Çelik, C. Bayındırlı and D. Erol, "Exergy, exergoeconomic, and sustainability analyses of a diesel engine using biodiesel fuel blends containing nanoparticles," *Energy*, vol. 274, no. 127278, 2023.
- [35] P. Tamilselvan, N. Nallusamy and S. Rajkumar, "A comprehensive review on performance, combustion and emission characteristics of biodiesel fuelled diesel engines," *Renewable and Sustainable Energy Reviews*, vol. 79, pp. 1134-1159, 2017.
- [36] L. Wang, Z. Zhao, C. Yu and H. Cui, "Experimental study of aviation kerosene engine with PJI system," *Energy*, Vols. 248., no. 123590, 2022.
- [37] X. Yang, W. Fan and R. Zhang, "Experimental investigations on aviation kerosene Multi-jets in high temperature and low pressure air crossflow," *Fuel*, vol. Volume 324, no. 124828, 2022.